Elastic scattering of low-energy electrons by boron trihalides

Márcio H. F. Bettega
Departamento de Física, Universidade Federal do Paraná, Caixa Postal 19081, 81531-990 Curitiba, Paraná, Brazil
(Received 27 July 1999; revised manuscript received 19 October 1999; published 2 March 2000)

We used the Schwinger multichannel method with pseudopotentials [Bettega *et al.*, Phys. Rev. A **47**, 1111 (1993)] to study elastic scattering of low-energy electrons by the boron trihalides BCl_3, BBr_3, and BI_3, at the static-exchange approximation. We calculated elastic integral, differential, and momentum transfer cross section from 5 to 50 eV. In particular, our integral cross section for BCl_3 agrees in shape with results of previous calculations by Isaacs *et al.* [Phys. Rev. A **58**, 2881 (1998)]. The symmetry decomposition of the integral cross section in the C_{2v} group is also presented. We discuss the existence of shape resonances for energies above 5 eV at the A_1, B_1, B_2, and A_2 symmetries. We also investigated the low-energy cross section for the B_2 symmetry for these three molecules. For BCl_3 our B_2 cross section shows good agreement with the results of Isaacs *et al.*

PACS number(s): 34.80.Bm

I. INTRODUCTION

Electron-molecule collision cross sections are an important piece of information in the description and understanding of the chemical processes that occur in cold plasmas. These plasmas have been widely used in processes of etching and chemical vapor deposition, which are important steps in the semiconductor fabrication [1]. However, the database on electron-molecule collision cross section is still modest, and a reliable cross section for molecules used as gas precursors is desired.

The boron trihalides BCl_3, BBr_3, and BI_3, have been used in these last few years as alternative gases in plasma etching processes [2]. Also, some experimental and theoretical studies on their electronic structure and properties have been carried out [3–6]. Only very recently Isaacs *et al.* calculated cross sections for e^--BCl_3 collision [7]. They covered energies from 0 eV up to 13 eV and presented results in both static-exchange and static-exchange plus polarization approximations. They studied the low-energy shape resonance at the B_2 symmetry and showed that its position moves from around 1.8 eV, in the static-exchange calculations to 0.25 eV, with the inclusion of polarization effects. Previous studies have found -0.4 eV (from the cross section for negative ion formation) [3] and -0.41 through -0.79 eV (values obtained with different basis sets and levels of approximation) [5] for the vertical electron affinity of BCl_3. Stockdale *et al.* [3] reported possible shape resonances near 2.5 eV and 8 eV. Tossell *et al.* [4] also found resonances in BCl_3 through the electron transmission spectroscopy very near threshold in B_2 symmetry, at 2.86 eV and 5.16 eV in A_1 symmetry and at 5.16 eV in B_1 symmetry; they also reported another two (possibly) core-excited shape resonances at 7.57 eV and 9.05 eV. Isaacs *et al.* also reported shape resonances for the A_1 symmetry, at 2.5 and 5.5 eV and for the B_1 symmetry, at 5.5 eV. However, for the other two molecules, BBr_3 and BI_3, there are no available calculated or measured cross sections.

In this work we present results of a fully *ab initio* calculation on e^--BCl_3, -BBr_3, and -BI_3 collision. We calculated elastic integral, differential, and momentum transfer cross sections for energies from 5 eV up to 50 eV. To perform these calculations we used the Schwinger multichannel (SMC) method with pseudopotentials (SMCPP) [8,9] at the static-exchange approximation. Along with the integral cross section for each one of these molecules we present its symmetry decomposition in the C_{2v} group, in order to investigate the structures that appear above 5 eV. We also calculated the cross section for the B_2 symmetry for energies lower than 5 eV, looking for low-energy shape resonances for BBr_3 and BI_3, in this particular symmetry.

The theoretical formulation of our method, the computational procedures used in our calculations, and our results and discussion will be presented in the next sections.

II. METHOD

Here we will describe the SMC [11,12] and SMCPP [8] methods. The SMC method is a multichannel extension of the Schwinger variational principle. Actually it is a variational approximation for the scattering amplitude, where the scattering wave function is expanded in a basis of $(N+1)$-particle Slater determinants

$$|\Psi_{\vec{k}}\rangle = \sum_m a_m^{\pm}(\vec{k})|\chi_m\rangle \tag{1}$$

and the coefficients $a_m^{\pm}(\vec{k})$ of this expansion are then variationally determined. The resulting expression for the scattering amplitude in the body frame is

$$[f_{\vec{k}_i,\vec{k}_f}] = -\frac{1}{2\pi}\sum_{m,n}\langle S_{\vec{k}_f}|V|\chi_m\rangle (d^{-1})_{mn}\langle\chi_n|V|S_{\vec{k}_i}\rangle, \tag{2}$$

where

$$d_{mn} = \langle\chi_m|A^{(+)}|\chi_n\rangle \tag{3}$$

and

$$A^{(+)}=\frac{\hat{H}}{N+1}-\frac{(\hat{H}P+P\hat{H})}{2}+\frac{(VP+PV)}{2}-VG_P^{(+)}V. \tag{4}$$

In the above equations $|S_{\vec{k}_i}\rangle$, the solution of the unperturbed Hamiltonian H_0, is the product of a target state and a plane wave, V is the interaction potential between the incident electron and the target, $|\chi_m\rangle$ is an $(N+1)$-electron Slater determinant used in the expansion of the trial scattering wave function, $\hat{H}=E-H$ is the total energy of the collision minus the full Hamiltonian of the system, with $H=H_0+V$, P is a projection operator onto the open-channel space defined by target eigenfunctions $|\Phi_l\rangle$

$$P=\sum_l^{open} |\Phi_l\rangle\langle\Phi_l|, \tag{5}$$

and $G_P^{(+)}$ is the free-particle Green's function projected on the P space.

For elastic scattering at the static-exchange approximation, the P operator is composed only by the ground state of the target $|\Phi_1\rangle$

$$P=|\Phi_1\rangle\langle\Phi_1| \tag{6}$$

and the configuration space $|\chi_m\rangle$ is

$$\{|\chi_m\rangle\}=\{\mathcal{A}|\Phi_1\rangle|\varphi_m\rangle\}, \tag{7}$$

where $|\varphi_m\rangle$ is a one-particle function represented by one molecular orbital and $\mathcal{A}$ is the antisymmetrization operator.

With the choice of Cartesian Gaussian functions to represent the molecular and scattering orbitals, all the matrix elements arising in Eq. (2) can be computed analytically, except those from $\langle\chi_m|VG_P^{(+)}V|\chi_n\rangle(VGV)$, that are evaluated by numerical quadrature [12].

The numerical calculation of the matrix elements from VGV represent the more expensive step in the SMC code and demand almost the entire computational time of the scattering calculation. These matrix elements are reduced to a sum of primitive two-electron integrals involving a plane wave and three Cartesian Gaussians

$$\langle\alpha\beta|V|\gamma\vec{k}\rangle=\int\int d\vec{r}_1 d\vec{r}_2 \alpha(\vec{r}_1)\beta(\vec{r}_1)\frac{1}{r_{12}}\gamma(\vec{r}_2)e^{i\vec{k}\cdot\vec{r}_2} \tag{8}$$

and must be evaluated for all possible combinations of α, β, and γ and for several directions and moduli of $\vec{k}$. We must also evaluate the one-electron integrals of the type

$$\langle\alpha|V^{PP}|\vec{k}\rangle=\int d\vec{r}\,\alpha(\vec{r})V^{PP}e^{i\vec{k}\cdot\vec{r}}. \tag{9}$$

These one-electron integrals are more complex than those involving the nuclei, but they can be calculated analytically and their number is also reduced due to the smaller basis set. In the above equation, V^{PP} is the nonlocal pseudopotential operator given by

$$\hat{V}^{PP}(r)=\hat{V}_{core}(r)+\hat{V}_{ion}(r), \tag{10}$$

with

$$\hat{V}_{core}(r)=-\frac{Z_v}{r}\left[\sum_{i=1}^{2} c_i^{core} erf[(\alpha_i^{core})^{1/2}r]\right], \tag{11}$$

and

$$\hat{V}_{ion}(r)=\sum_{n=0}^{1}\sum_{j=1}^{3}\sum_{l=0}^{2} A_{njl}r^{2n}e^{-\alpha_{jl}r^2}\sum_{m=-l}^{+l}|lm\rangle\langle lm|, \tag{12}$$

where Z_v is the valence charge of the atom and in this application it is equal to 3 for B, and 7 for Cl, Br, and I. The coefficients c_i^{core}, A_{njl}, and the decay constants α_i^{core} and α_{jl} are tabulated in Ref. [10].

Even for small molecules, a large number of the two-electron integrals must be evaluated. This limits the size of molecules in scattering calculations. In the SMCPP method we need a shorter basis set to describe the target and scatter-

TABLE I. Cartesian Gaussian function exponents for boron and halogens.

Type	B Exponent	Cl Exponent	Br Exponent	I Exponent	Coefficient
s	7.743009	9.284428	6.779740	4.497056	1.0
s	1.588291	1.845608	1.071059	1.034061	1.0
s	0.385169	0.449968	0.748707	0.586050	1.0
s	0.118779	0.170020	0.202254	0.229555	1.0
s	0.026184	0.008157	0.036220	0.036150	1.0
p	3.487316	2.344123	4.789276	4.343653	1.0
p	1.118566	0.902071	1.856547	1.065825	1.0
p	0.398653	0.345005	0.664700	0.365993	1.0
p	0.144251	0.120979	0.265909	0.118764	1.0
p	0.050830	0.027029	0.098552	0.028456	1.0
d	0.382078	1.554031	0.477153	0.267526	1.0
d	0.100241	0.311512	0.139024	0.093270	1.0

TABLE II. Relation between the symmetries of C_{2v} and D_{3h} groups.

C_{2v}	D_{3h}
a_1	$a_1'+e'$
b_1	$a_2'+e'$
b_2	$a_2''+e''$
a_2	$a_1''+e''$

ing and consequently the number of two-electron integrals is smaller than in the all-electron case. The reduction in the number of these integrals allows the study of larger molecules than those reachable by all-electron techniques.

We used the pseudopotentials of Ref. [10] in order to describe the core electrons of the boron and the halogens. The basis functions used in the calculations are shown in Table I, and were obtained as described in Ref. [13]. The scattering basis functions are separated by symmetry as follows: 44 for A_1, 31 for B_1, 21 for B_2, and 12 for A_2. We have not included in our calculations the combination $[(x^2+y^2+z^2)\exp(-\alpha r^2)]$ in order to avoid linear dependency in the basis set. We have tested the convergence of our cross sections with respect to the size of the basis set using a large basis. This basis set is obtained from the basis shown in Table I by including one *s*-type function and one *p*-type function in each center. The results obtained with these two sets differ by about 5% or less.

Although these molecules belong to the D_{3h} group, our calculations were performed in the C_{2v} group. In Table II we present the relation between the symmetries of these two groups. The experimental bond lengths used in our calculations are shown in Table III [14].

III. RESULTS AND DISCUSSION

Figure 1(a) shows our calculated integral cross section (ICS) for BCl_3 and also static-exchange results for BCl_3 of Ref. [7], obtained with the complex Kohn method. Although the two calculations agree in shape, the complex Kohn results lie below ours and the positions of their structures are shifted to higher energies, in comparison with ours. Isaacs *et al.* have included in their calculations continuum numerical functions retaining terms up to $\ell=5$. These partial waves were then used to get their cross sections. We have also calculated the integral cross section in the angular momentum representation truncating the partial wave expansion of the scattering amplitude at $\ell=5$, 6, and 7. These results are also shown in Fig. 1(a). Our cross section obtained with partial waves up to $\ell=6$ agrees in magnitude with the cross section of Isaacs *et al.*, but their structures remain shifted to the right, when compared with ours. Another possible reason

TABLE III. Experimental bond length $[r(\text{B-X})]$ (Å) for BX_3.

	BCl_3	BBr_3	BI_3
r(B-X)	1.742	1.893	2.118

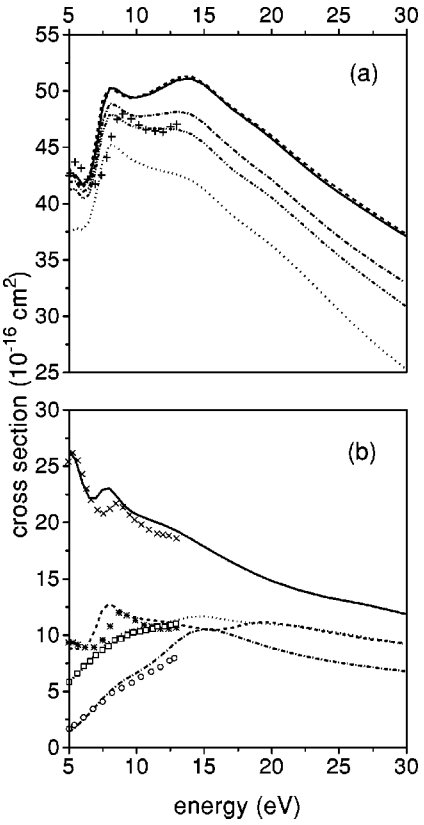

FIG. 1. (a) Elastic integral cross sections for BCl_3. Solid line, SMCPP results for the basis set of Table I and at $r(\text{B-Cl})=1.742$ Å; dashed line, SMCPP results for the basis set of Table I at $r(\text{B-Cl})=1.754$ Å; dotted line, our results from partial wave expansion up to $\ell=5$; dashed-dotted-dotted line, our results from partial wave expansion up to $\ell=6$; dashed-dotted line, our results from partial wave expansion up to $\ell=7$; crosses, complex Kohn results of Ref. [7]. (b) Symmetry decomposition of the integral cross section. Solid line, our A_1 cross section; crosses, A_1 cross section of Isaacs *et al.*; dashed line, our B_1 cross section; stars, B_1 cross section of Isaacs *et al.*; dotted line, our B_2 cross section; squares, B_2 cross section of Isaacs *et al.*; dashed-dotted line, our A_2 cross section; circles, A_2 cross section of Isaacs *et al.*

for this discrepancy could be the different bond lengths used in both calculations. We used $r(\text{B-Cl})=1.742$ Å in the present calculation, and Isaacs *et al.* used $r(\text{B-Cl})=1.754$ Å, in their complex Kohn calculations. In order to investigate this possibility we also calculated ICS at $r(\text{B-Cl})=1.754$ Å, with the basis set shown in Table I. The results are also shown in Fig. 1(a), and the cross sections obtained with different bond lengths are quite similar. The difference in magnitude between our cross section and the cross section of Isaacs *et al.* could be explained by a lack of convergence in the partial wave expansion by Isaacs *et al.* The shift in the structures remains to be explained. In order to find which symmetries are responsible for the discrepancy seen in Fig. 1(a), we show in Fig. 1(b) the symmetry decomposition of the integral cross section for BCl_3. We compare our results with the results of Isaacs *et al.* The difference seen in the integral cross section comes primarily from the A_1, B_1, and A_2 symmetries. In particular, our structures at the A_1 and B_1

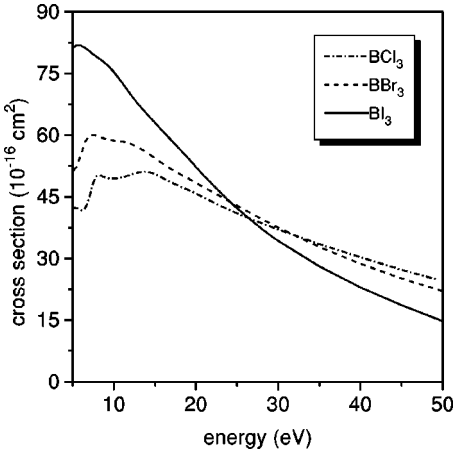

FIG. 2. Elastic integral cross sections for BX_3.

symmetries are shifted to lower energies and are greater in magnitude.

Figure 2 shows our integral cross sections for the boron trihalides. Comparing the cross sections of BX_3, one can see that for energies from 5 eV up to 20 eV the magnitude of the cross sections is ordered as follows: $\sigma_{BCl_3}<\sigma_{BBr_3}<\sigma_{BI_3}$. Above 20 eV there is a crossing between the curves and the previous relation changes to $\sigma_{BCl_3}>\sigma_{BBr_3}>\sigma_{BI_3}$. The ICS for BCl_3 and BBr_3 are very similar in shape, and present bumps around 10 eV and 15 eV. In this energy range, the ICS of BI_3 seems to be structureless.

In order to better understand the behavior of the ICS of these three molecules we made their symmetry decomposition in the C_{2v} group, and the results are shown in Fig. 3. We also present the total cross section. The A_1 and B_1 cross section for BCl_3 and BBr_3 present a bump above 5 eV. We also calculated the eigenphase sum for each one of these symmetries and although not shown here, we found that these bumps are in fact shape resonances, as pointed out by Isaacs *et al.* [7]. The A_1 and B_1 resonances occur at the same energy, $E\sim 8$ eV for BCl_3 and $E\sim 7$ eV for BBr_3, and can be attributed to the twofold degenerate E' symmetry of the D_{3h} group, that splits into the A_1 and B_1 symmetries of the C_{2v} group, as shown in Table II. For BCl_3, Tossell *et al.* reported a resonance in E' symmetry at 5.16 eV. Isaacs *et al.*, including polarization effects, reported this resonance at 5.5 eV, which compares quite well with the predictions of Tossell *et al.* Stockdale *et al.* reported resonances at 2.5 eV and at 8 eV. We have also found very broad shape resonances for the B_2 and A_2 symmetries, but now for all three molecules. For each one of these molecules, the A_2 and B_2 resonances also occur at the same energy, $E\sim 15$ eV for BCl_3, $E\sim 13$ eV for BBr_3, and $E\sim 10$ eV for BI_3, and can be attributed to the twofold degenerate E'' of the D_{3h} group, that now splits into the A_2 and B_2 symmetries of the C_{2v} group, as also shown in Table II. These broad structures in the A_2 and B_2 have not been seen by Isaacs *et al.* once they presented static-exchange results just up to 13 eV.

As pointed out by Isaacs *et al.* in their study on e^--BCl_3 collision, the main feature of its ICS at low impact energies is the B_2 shape resonance (that is associated to the A_2'' symmetry of the D_{3h} group). They included polarization effects to get a more precise description of its position: from 1.8 eV at the static-exchange approximation to 0.25 eV including polarization effects. Tossell *et al.* reported a shape resonance

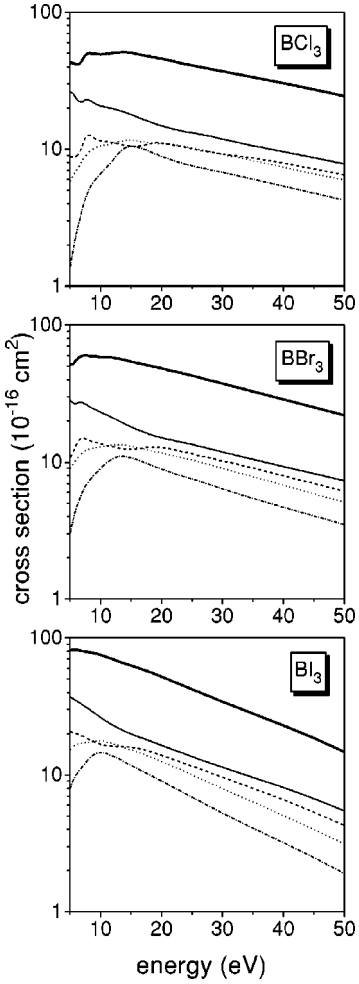

FIG. 3. Symmetry decomposition of the integral cross section of BX_3. A_1 symmetry, solid line; B_1 symmetry, dashed line; B_2 symmetry, dotted line; A_2 symmetry, dotted-dashed line; sum, thick solid line.

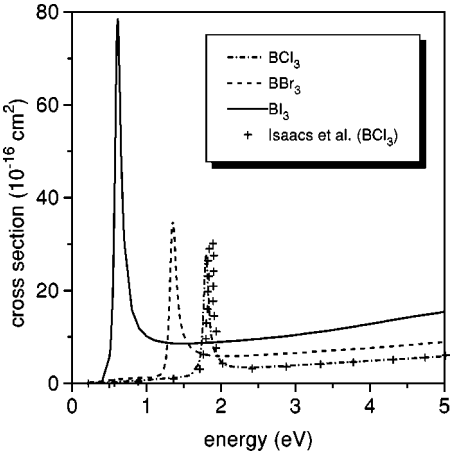

FIG. 4. B_2 integral cross section for BX_3. The crosses are results from Ref. [7].

TABLE IV. Calculated vertical electron affinities (VEA) and virtual orbital canonical energies (VO) (eV) for BX_3.

	BCl_3	BBr_3	BI_3
VEA	−0.82	−0.25	+0.61
VO	1.51	1.48	0.64
	2.06	4.14	1.98

for this symmetry near 0 eV. We also investigated the low-energy behavior of the B_2 static-exchange cross section for the BX_3 molecules, and the results are shown in Fig. 4, along with the B_2 static-exchange results of Isaacs *et al.* All molecules present a sharp structure and, in particular, our results for BCl_3 agree with those of Isaacs *et al.*, although our resonance is shifted to lower energies, following the behavior of the A_1 and B_1 (E') resonances, as discussed above. The peaks are located at $E\sim1.8$ eV, for BCl_3, $E\sim1.34$ eV, for BBr_3, and $E\sim0.61$ eV, for BI_3. In Table IV we show the energies of the first and the second canonical Hartree-Fock virtual orbitals, obtained with the basis set of Table I, and related with the first two unoccupied orbitals of the B_2 symmetry for BX_3. The first energy, for BBr_3 and BI_3, is quite close to the position of these peaks. For BCl_3, the first and the second energies are very close to the energy of the peak. We also show in Table IV the vertical electron affinity for these molecules, obtained as the difference of the Hartree-Fock energies of the neutral molecule and the anion using the pseudopotentials of Ref. [10] and the basis set of Table I. The ground state of the negative ions of BCl_3 and BBr_3, calculated at the experimental geometry of the ground state of the neutral molecules, lies above the ground state of the neutral molecule. For BI_3, however, this number is positive; that is, the ground state of the anion lies below the ground state of the neutral molecule. Based on these results, we expect that with the inclusion of polarization effects the B_2 structure of BI_3 will vanish. For BBr_3, in principle, this resonance should move down in energy.

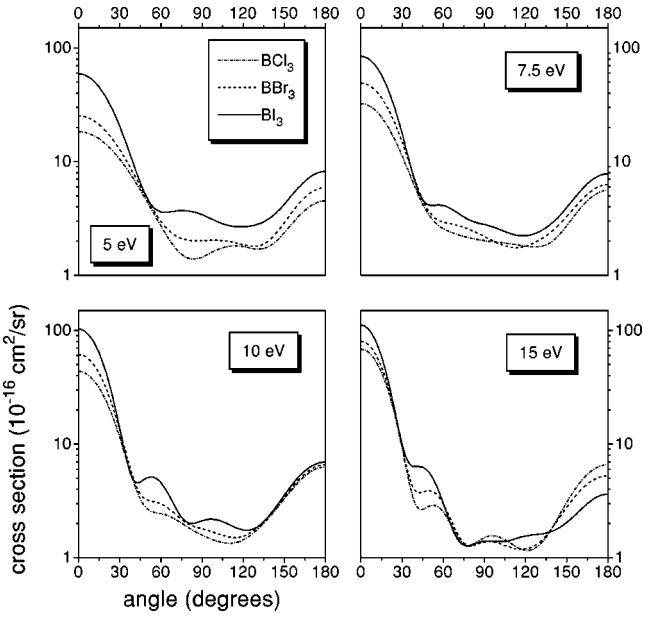

FIG. 5. Differential cross section for BX_3 at 5, 7.5, 10, and 15 eV.

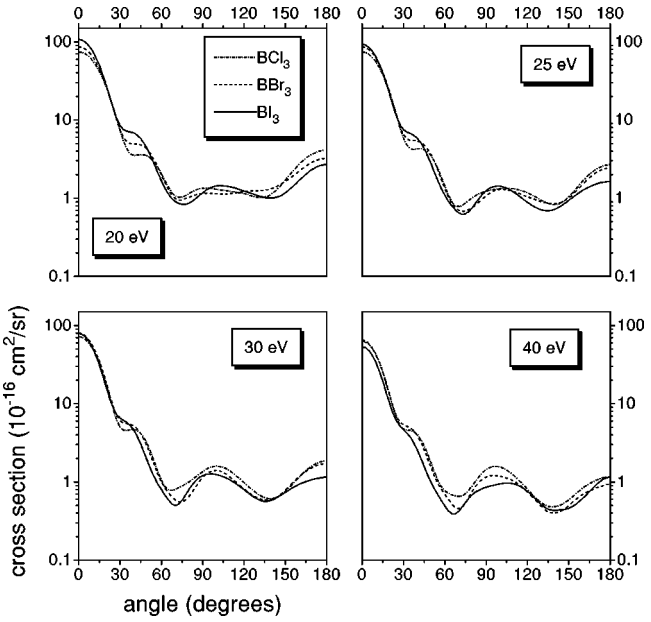

FIG. 6. Differential cross section for BX_3 at 20, 25, 30, and 40 eV.

It should be noted that at very low energies, a shape resonance may appear as a series of vibrational peaks in the total cross section [15]. In this case, a fixed-nuclei calculation, even with the inclusion of polarization effects, does not give a correct description of the resonance.

Figures 5 and 6 show the differential cross sections (DCS) for BX_3 at 5, 7.5, 10, 15, 20, 25, 30, and 40 eV. The oscillations starting at 10 eV for BI_3, and at 15 eV for BCl_3 and BBr_3 in the DCS indicate high partial wave coupling. For energies above 20 eV the shape of the DCS for the BX_3 molecules is very similar. In Fig. 7 we show momentum transfer cross sections (MTCS) for BX_3 (X=Cl, Br, I). The same behavior seen in the ICS also can be seen in the MTCS plot, but with the crossing occurring at 15 eV.

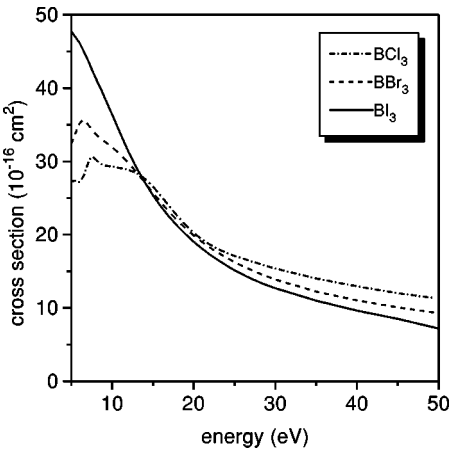

FIG. 7. Momentum transfer cross section for BX_3.

IV. SUMMARY

We presented cross sections for elastic scattering of low-energy electrons by BX_3 (X=Cl, Br, I). For energies below 25 eV we found that the magnitude of the integral cross sections of these boron trihalides follows the order $\sigma_{BCl_3} < \sigma_{BBr_3} < \sigma_{BI_3}$. Around 25 eV there is a crossing between the curves and the order changes to $\sigma_{BCl_3} > \sigma_{BBr_3} > \sigma_{BI_3}$. Through the symmetry decomposition of the integral cross sections in the C_{2v} group, we found resonances at A_1 and B_1 symmetries, for BCl_3 and BBr_3, and at the A_2 and B_2 symmetries, for all BX_3 molecules. We also investigated the low-energy B_2 cross sections for these molecules and found a very pronounced peak in these cross sections. For BI_3, however, once its vertical electron affinity is positive, we expect that this resonance will vanish with the inclusion of polarization effects.

ACKNOWLEDGMENTS

The author acknowledges support from the Brazilian agency Conselho Nacional de Desenvolvimento Científico e Tecnológico (CNPq). The author thanks Professor Marco A. P. Lima, Professor Luiz G. Ferreira, Professor Vincent McKoy, Dr. Carl Winstead, and Mr. Márcio T. do N. Varella for fruitful discussions. These calculations were performed at CENAPAD-SP, CENAPAD-NE, and at CCE-UFPR. The author also acknowledges the use of the IBM-SP2 at CACR-Caltech.

[1] V. McKoy, C. Winstead, and C-H. Lee, J. Vac. Sci. Technol. A **16**, 324 (1998).

[2] J. J. Wang, H. Cho, J. R. Childress, S. J. Pearton, F. Sharifi, K. H. Dahmen, E. S. Gillman, Plasma Chem. Plasma Process. **19**, 229 (1999); J. Hong, J. A. Caballero, E. S. Lambers, J. R. Childress, and S. J. Pearton, J. Vac. Sci. Technol. B **16**, 3349 (1998); J. Hong, H. Cho, T. Maeda, C. R. Abernathy, S. J. Pearton, R. J. Shul, and W. S. Robson, *ibid.* **16**, 2690 (1998); H. Cho, J. Hong, T. Maeda, S. M. Donovan, J. D. MacKenzie, C. M. Abenathy, S. J. Pearton, R. J. Shul, and J. Han, MRS Internet J. Nitride Semicond. Res. **3**, 5 (1998).

[3] J. A. Stockdale, D. R. Nelson, F. J. Davis, and R. N. Compton, J. Chem. Phys. **56**, 3336 (1972).

[4] J. A. Tossell, J. H. Moore, and J. K. Olthoff, Int. J. Quantum Chem. **29**, 1117 (1986).

[5] K. K. Baeck and R. J. Bartlett, J. Chem. Phys. **106**, 4604 (1997).

[6] L. G. Shpinkova, D. M. P. Holland, and D. A. Shaw, Mol. Phys. **96**, 323 (1999); R. I. Keir and G. L. D. Ritchie, Chem. Phys. Lett. **290**, 409 (1998); H. Biehl, D. M. Smith, R. P. Tuckett. K. R. Yoxall, H. Baumgartel, H. W. Jochims, and U. Rokland, Mol. Phys. **87**, 1199 (1996).

[7] W. A. Isaacs, C. W. McCurdy, and T. N. Rescigno, Phys. Rev. A **58**, 2881 (1998).

[8] M. H. F. Bettega, L. G. Ferreira, and M. A. P. Lima, Phys. Rev. A **47**, 1111 (1993).

[9] M. H. F. Bettega, M. A. P. Lima, and L. G. Ferreira, J. Phys. B **31**, 2091 (1998); M. H. F. Bettega, L. G. Ferreira, and M. A. P. Lima, Phys. Rev. A **57**, 4987 (1998); S. M. S. da Costa and M. H. F. Bettega, Eur. Phys. J. D **3**, 67 (1998); M. H. F. Bettega, M. T. do N. Varella, L. G. Ferreira, and M. A. P. Lima, J. Phys. B **31**, 4419 (1998); A. P. P. Natalense, L. G. Ferreira, and M. A. P. Lima, Phys. Rev. Lett. **81**, 3832 (1998); A. P. P. Natalense, M. H. F. Bettega, L. G. Ferreira, and M. A. P. Lima, Phys. Rev. A **59**, 879 (1999); M. T. do N. Varella, M. H.F. Bettega, A. J. R. da Silva, and M. A. P. Lima, J. Chem. Phys. **110**, 2452 (1999).

[10] G. Bachelet, D. R. Hamann, and M. Schlüter, Phys. Rev. B **26**, 4199 (1982).

[11] K. Takatsuka and V. McKoy, Phys. Rev. A **24**, 2473 (1981); **30**, 1734 (1984).

[12] M. A. P. Lima, L. M. Brescansin, A. J. R. da Silva, C. Winstead, and V. McKoy, Phys. Rev. A **41**, 327 (1990).

[13] M. H. F. Bettega, A. P. P. Natalense, M. A. P. Lima, and L. G. Ferreira, Int. J. Quantum Chem. **60**, 821 (1996).

[14] *CRC Handbook of Chemistry and Physics*, 79th ed., edited by D. R. Lide (CRC Press, Boca Raton, FL, 1998).

[15] R. J. Gulley, S. L. Lunt, J-P. Ziesel, and D. Field, J. Phys. B **31**, 2735 (1998).